Reaction-diffusion models of decontamination

Problem presented by

Harry McEvoy

Dstl

Executive Summary

A contaminant, which also contains a polymer is in the form of droplets on a solid surface. It is to be removed by the action of a decontaminant, which is applied in aqueous solution. The contaminant is only sparingly soluble in water, so the reaction mechanism is that it slowly dissolves in the aqueous solution and then is oxidized by the decontaminant. The polymer is insoluble in water, and so builds up near the interface, where its presence can impede the transport of contaminant. In these circumstances, Dstl wish to have mathematical models that give an understanding of the process, and can be used to choose the parameters to give adequate removal of the contaminant. Mathematical models of this have been developed and analysed, and show results in broad agreement with the effects seen in experiments.

Version 1.1
30 April 2009

Report authors

David Allwright (Knowledge Transfer Network for Industrial Mathematics)
Maurice Blount (University of Cambridge)
Heike Gramberg (University of Oxford)
Ian Hewitt (University of Oxford)

Contributors

Abdulhadi Aminu (University of Birmingham)
Chris Breward (University of Oxford)
Piotr Broda (University of Warsaw)
John Byatt-Smith (University of Edinburgh)
Chris Catt (University of Southampton)
Nawinda Chutsagulprom (University of Oxford)
Joe Fehribach (WPI)
Heike Gramberg (University of Oxford)
Ian Hewitt (University of Oxford)
Roslyn Hickson (UNSW@ADFA)
Poul Hjorth (Technical University of Denmark)
Cara Morgan (University of Oxford)
Rafael Morones (Instituto Tecnológico Autónomo de México)
John Ockendon (University of Oxford)
Colin Please (University of Southampton)
Tim Reis (University of Oxford)
David Sibley (University of Bath)
Peter KinPo Tam (University of Birmingham)
Alice Thompson (University of Nottingham)

ESGI68 was jointly organised by
The University of Southampton
The Knowledge Transfer Network for Industrial Mathematics

and was supported by
The Engineering and Physical Sciences Research Council

Contents

1 Introduction

Dstl is the main research organisation of the Ministry of Defence. The problems described here are part of the remit of the Hazard Management team. Their brief is to develop methods to minimize the hazard resulting from the use of chemical, biological or radiological weapons. The team's activities support both civil and military hazard management. For instance, patented decontamination formulations have been evaluated for uses such as cleaning railway rolling stock, removal of traffic film from road vehicles, and graffiti removal.

1.1 Problem description

(1.1.1) Consider a polymer solution for which the solvent is a pollutant, which we call A throughout (the Agent of contamination). A drop on a horizontal surface will adopt an equilibrium shape determined by its size and surface tension and gravity, in a time determined by its viscosity. If a layer of decontaminant, a solution of B in water, is applied above, then A will diffuse into the aqueous layer and undergo a chemical reaction with B which renders it harmless. The polymer P does not diffuse into the aqueous layer. This situation is illustrated in Figure 1.

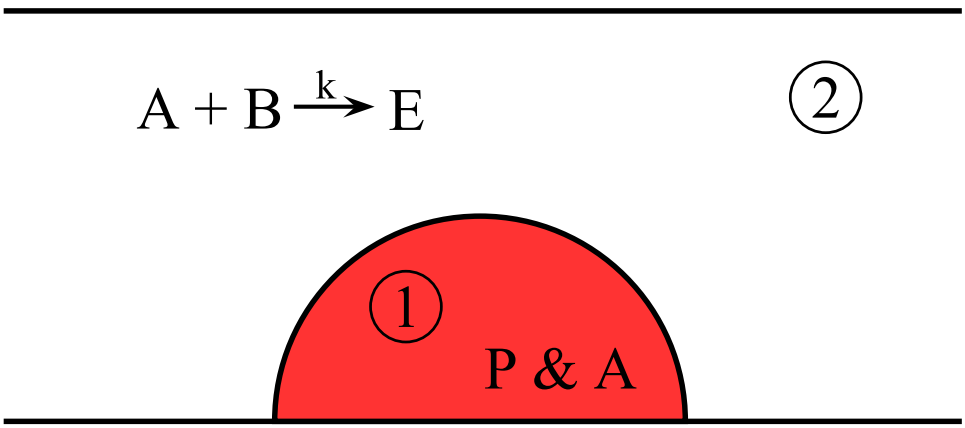

- A: contaminant
- B: decontaminant (2% mass fraction)
- P: polymer (5% mass fraction)

Figure 1: Schematic diagram

(1.1.2) In some cases, the aqueous layer may contain a microemulsion of toluene and butanol. This has three effects. First, it increases the solubility of A in the aqueous layer, which makes it easier for the required reaction to

occur. Second, it decreases the effective concentration of B in the aqueous layer, which reduces the reaction rate (or increases the amount of B that is required). And third, the organic component can enter the A region, where it can cause the polymer to swell.

(1.1.3) The diffusion coefficients in the polymer solution depend on the polymer concentration, and so do the surface tension and viscosity.

(1.1.4) In some cases there may be some absorption of A into the solid surface, for instance if it is porous like concrete.

(1.1.5) The challenge is to determine the residual pollution level left on the surface as a function of time, and of all the physical parameters such as drop size, initial concentrations, reaction constants *etc.*

(1.1.6) A second problem is to consider the same droplet but deposited on a vertical surface. In this case the decontaminant is delivered as a spray. There is gravity-driven flow of the decontaminant solution down the surface, which brings fresh decontaminant solution into contact with each drop, but also limits the contact time. Again, the question is how to determine the total required volume, and the time to deliver that volume, given the relevant physical and chemical properties.

2 Mathematical models

We describe the models and their relationships here.

2.1 Common features of all models

(2.1.1) All of our models will assume

(a) linear diffusion of A and B in the reaction layer, each with constant diffusivity;

(b) simple law-of-mass-action kinetics with a 1:1 mole ratio between A and B;

(c) no transport of A into the solid substrate;

(d) no transport of A or B or water from the top of the applied layer (in particular, no evaporation);

(e) no diffusion of B into the contamination drop;

(f) no diffusion of P into the reaction layer;

(g) except in Section 2.7 we assume there are no advective velocities in the fluids, so all mass transport is by diffusion;

(h) no volume changes on mixing, so since we assume all densities are effectively 1, we have conservation of volume.

(2.1.2) None of the models consider in detail the case of the microemulsion that was mentioned in paragraph (1.1.2).

2.2 Basic one-dimensional model

(2.2.1) Dstl's simplest model for the droplet shape is a spherical cap with angle of contact α of 20–25°. This has an aspect ratio (radius:thickness) of about 5. ($h/r = \tan(\alpha/2)$ is 0.2 for $\alpha \approx 22.6°$.) In view of this, it was decided to consider a 1-dimensional problem first, which we could think of as modelling the diffusion and reaction in the vertical direction above the centre of the drop.

(2.2.2) We consider a lower contaminant layer, initially consisting of A mixed uniformly with polymer P, and initially of thickness h_0. We consider an applied upper layer of thickness $H - h_0$ that is a uniform solution of the decontaminant B. The situation is shown for the case of no polymer in Figure 2, and for the case with polymer present in Figure 3.

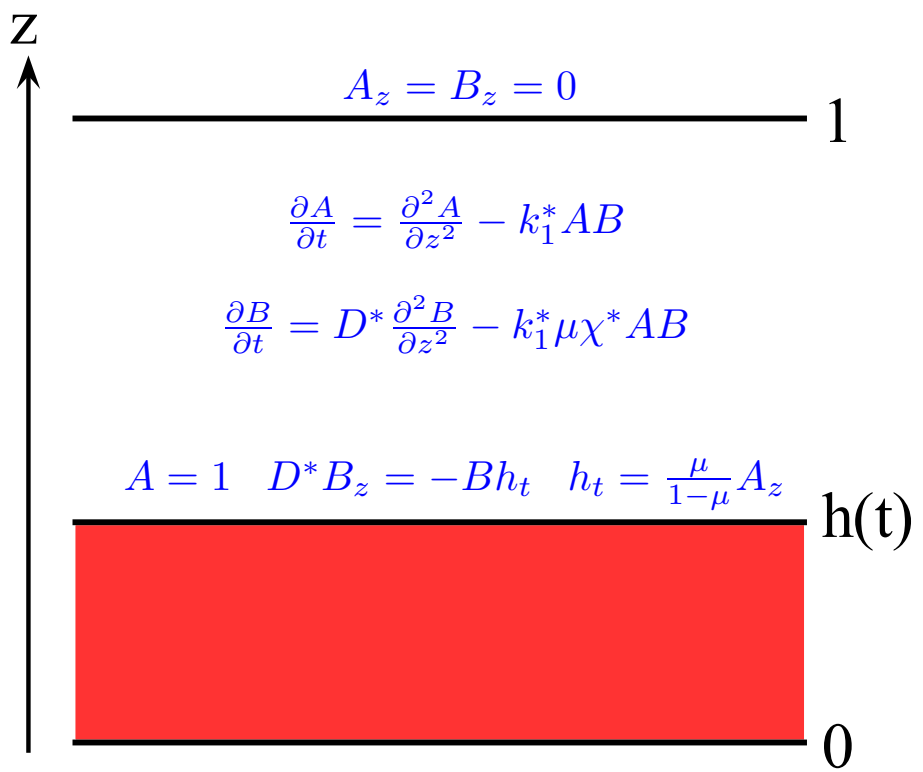

Figure 2: Configuration of one-dimensional model with no polymer. The equations are given in scaled variables as defined in Section 2.4.

The process to be modelled then consists of A diffusing from the lower layer into the upper and reacting with B, with the result that each layer becomes non-uniform.

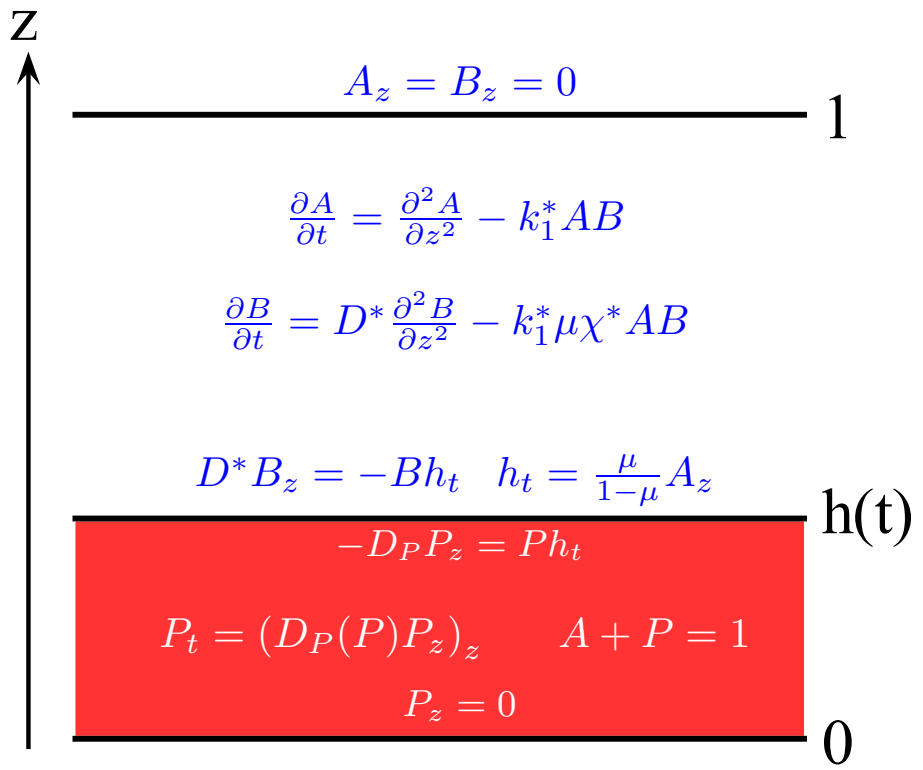

Figure 3: Configuration of one-dimensional model with polymer. The equations are given in scaled variables as defined in Section 2.4.

(2.2.3) We take layer 1 to occupy $0 < z < h(t)$, and to have concentration $P(z,t)$ of polymer and $A(z,t)$ of contaminant, and we treat these as being mass fractions so that $A + P = 1$. We think first of the polymer as being dilute enough that it can be modelled by a diffusion process

$$\frac{\partial P}{\partial t} = \frac{\partial}{\partial z}\left(D_p \frac{\partial P}{\partial z}\right), \tag{1}$$

with diffusivity D_p that may depend on P. The boundary conditions representing the facts that P cannot penetrate the lower boundary or the upper are

$$\frac{\partial P}{\partial z} = 0 \text{ at } z = 0; \quad -D_P \frac{\partial P}{\partial z} = P\dot{h} \text{ at } z = h. \tag{2}$$

This, combined with $A + P = 1$ means that we also have a diffusive flux of A in layer 1, also with diffusivity D_P. We shall use D_{A1} to denote this effective diffusivity of A in the lower layer.

(2.2.4) We take layer 2 to occupy $h(t) < z < H$, and to have concentrations $A(z,t)$ of contaminant and $B(z,t)$ of reagent, which are both dilute. We take A and B both to be mass fractions also, and we are regarding the densities of the two layers as being equal. The reaction we take in the form

$$\text{A+B} \rightarrow \text{E (reaction products)},$$

so we assume its rate is k_1AB. Since A and B are in dilute aqueous solution we model their diffusion by constant diffusion coefficients D_A and D_B, so we have

$$\frac{\partial A}{\partial t} = D_A \frac{\partial^2 A}{\partial z^2} - k_1 AB, \qquad \frac{\partial B}{\partial t} = D_B \frac{\partial^2 B}{\partial z^2} - k_1 AB. \tag{3}$$

(2.2.5) At the interface $z = h(t)$ between layers 1 and 2, we assume that thermodynamic equilibrium of A is reached instantaneously, and so the condition determining the interface velocity $\dot{h}$ is the mass transport of A across the interface. The equations representing these conditions are

$$A(h+) = \mu A(h-), \tag{4}$$

$$-D_A \left.\frac{\partial A}{\partial z}\right|_{h+} - A(h+)\dot{h} = -D_{A1} \left.\frac{\partial A}{\partial z}\right|_{h-} - A(h-)\dot{h}. \tag{5}$$

In the units we are using, the partition coefficient μ is the solubility of A in the upper layer expressed as a mass fraction, since when the upper layer is in equilibrium with pure A in the lower layer, $A(h-) = 1$ and $A(h+) = \mu$. There is no transport of B across the interface, so

$$-D_B \frac{\partial B}{\partial z} - B\dot{h} = 0 \text{ at } z = h. \tag{6}$$

(2.2.6) Finally, there is no mass transport of A or B across the upper interface, so

$$\frac{\partial A}{\partial z} = 0, \quad \frac{\partial B}{\partial z} = 0 \text{ at } z = H. \tag{7}$$

(2.2.7) The initial concentrations we take to be $P = P_0$ and $A = A_0 = 1 - P_0$ in the lower layer, and $B = B_0$ and $A = 0$ in the upper layer.

(2.2.8) When A diffuses out of the lower layer in this model, the concentration of P will rise near the interface, and it is questionable whether the diffusion model in equation (1) will be appropriate. Ideally we would like a model for the diffusion in this layer that is valid over the whole range of proportions of A to P. In the next two paragraphs, we describe two alternative possible approaches to obtaining such a model.

(2.2.9) There are models for the diffusion of a molecule, A in our case, through a polymer solution at low concentrations of A. The paper [1] reviews these models. One due to Phillies takes the diffusivity in the form

$$D = D_0 \exp(-\alpha c^\nu), \tag{8}$$

where D_0 is the low-concentration limit, c is the concentration of polymer, α depends on the molecular weight M_A of A and is estimated as proportional to M_A^β with $0.8 < \beta < 1$ for a polymer, or R_h^δ with $0 < \delta < 0.2$ for

smaller molecules, where R_h is the hydraulic radius of the molecule. The exponent ν is expected to vary from 0.5 for a polymer to 1 for smaller molecules.

(2.2.10) A different approach is to use a full two-phase flow model for P and A, with mass conservation, force balance (for the quasistatic situation of slow flow), and with a suitable model for interaction force between A and P. Such models have been developed in various contexts, including the mathematical modelling of ice cream, as reported in [2].

2.3 Numerical results from one-dimensional model

(2.3.1) The model above can be solved numerically. In each layer, a scaling depending on $h(t)$ is used to replace the layer by a fixed interval $(0, 1)$. This results in an advection-reaction-diffusion system, which can be solved by an up-winding method.

(2.3.2) Some results from this are shown in Figures 4-6. First, results with no polymer present are in Figure 4.

(2.3.3) Corresponding results with polymer present in layer 1 are shown in Figure 5. Here the polymer has a diffusivity such that it does build up near the interface, but the concentration does not rise to more than 15%. However, in Figure 6 the diffusivity of the polymer is set lower (and more realistic), and here the concentration does built up to nearly 100% near the interface, which slows down the diffusion of A into the reacting layer, and so slows the reaction rate very much.

(2.3.4) The way that the polymer is swept up by the interface moving downwards was also studied. The length scale of the sweep-up is $D_P/|\dot{h}|$. If D_P is constant, the solution can be studied analytically by converting the equation into a Volterra integral equation for the value of P at $z = h(t)$. However, to calculate P this way for general motion of $h(t)$ would still require numerical solution, and this approach has not been pursued.

2.4 Analysis of the one-dimensional model with no polymer

(2.4.1) When there is no polymer, the concentration of A in the lower layer is constantly equal to its initial value $A_0 = 1$. So the concentration of A at the interface is constantly equal to the solubility μ, until the layer thickness h reduces to 0. So the motion of the interface $\dot{h}$ is coupled to the boundary conditions on A and B by

$$-D_B B_z/B = \dot{h} = D_A A_z/(1-\mu) \text{ at } z = h. \tag{9}$$

(2.4.2) If we rescale these equations by scaling z and h with H, B with B_0 (the initial concentration), t with H^2/D_A, and A with μ, then we obtain the

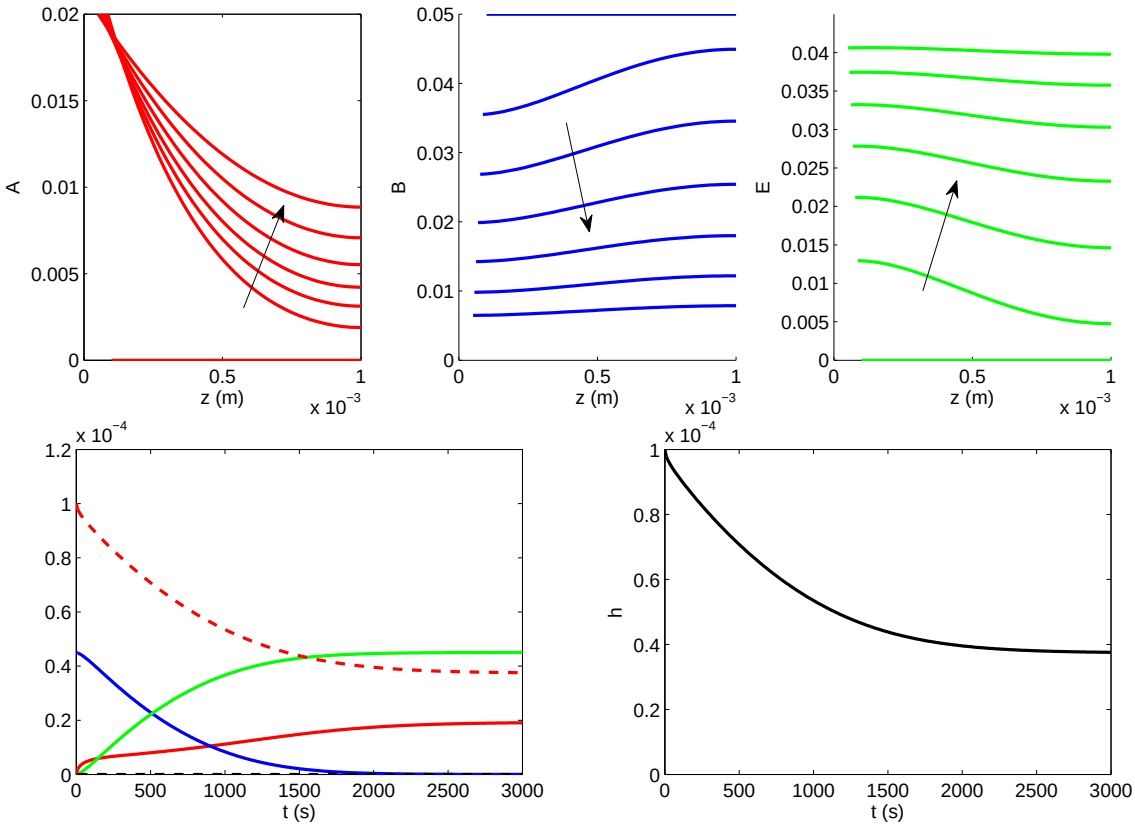

Figure 4: Using $\mu = 0.02$, $D_A = D_B = 10^{-9}$ m^2 s^{-1}, $H = 1$ mm, $h = 0.1$ mm, $B_0 = 5\%$, $k_1 B_0 = 0.01$ (so $D^* = 1$, $\chi^* = 20$, $k_1^* = 10$). Polymer not included. Profiles are shown at intervals of 3 minutes. Time profiles show total volume of A in decontaminant layer (solid red), A in polymer layer (dashed red), B (blue), E (green), P (dashed black). Reactions are largely exhausted due to B reducing to 0.

system

$$A_t = A_{zz} - k_1^* AB, \qquad B_t = D^* B_{zz} - k_1^* \mu \chi^* AB, \tag{10}$$

with

$$k_1^* = k_1 B_0 H^2 / D_A = \frac{\text{diffusion time scale}}{\text{reaction time scale}}, \tag{11}$$

and $D^* = D_B/D_A$, the diffusivity ratio, which is of order 1. The boundary conditions in these variables are

$$A = 1, \quad \dot{h} = \frac{\mu}{1-\mu} A_z = -D^* B_z / B \text{ at } z = h, \tag{12}$$

where

$$\chi^* = A_0/B_0. \tag{13}$$

(2.4.3) These equations can be analysed for small μ and times of order $1/\mu$ if $k_1^* \chi^*$

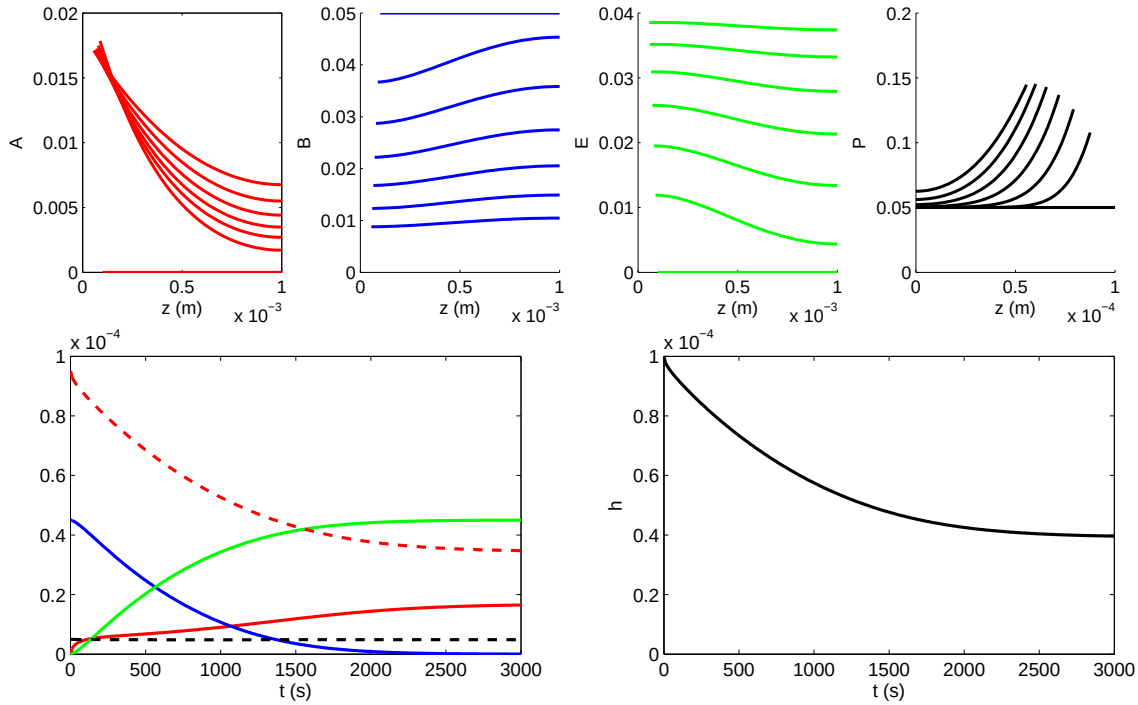

Figure 5: As in Figure 4, but including an initial 5% polymer in the contaminant layer which diffuses with diffusion coefficient $D_P = 10^{-12}$ m^2 s^{-1}.

is of order 1. We rescale time to $\tau = t\mu$, then the B equation becomes

$$\frac{\partial B}{\partial \tau} = \frac{D^*}{\mu}\frac{\partial^2 B}{\partial z^2} - k_1^* \chi^* A B, \tag{14}$$

so for small μ we have $B_{zz} = 0$ to leading order. However, $B_z = 0$ at $z = 1$ and $B_z = -\mu(dh/d\tau)B/D^*$ is also 0 to leading order, so B is a function of τ only, $B = \overline{B}(\tau)$. Integrating the B equation through the layer $h < z < 1$ and using the upper and lower boundary conditions then gives

$$(1-h)\overline{B}_\tau = \overline{B}h_\tau - k_1^*\chi^*\overline{B}\int_h^1 A\,dz. \tag{15}$$

The A equation then is $A_{zz} = k_1^*\overline{B}A$ to leading order, so with the boundary conditions of $A_z = 0$ at $z = 1$ and $A = 1$ at $z = h$ we have

$$A = \frac{\cosh\left((k_1^*\overline{B})^{1/2}(1-z)\right)}{\cosh\left((k_1^*\overline{B})^{1/2}(1-h)\right)}. \tag{16}$$

This then gives the velocity of the interface to leading order as

$$h_\tau = -(k_1^*\overline{B})^{1/2}\tanh\left((k_1^*\overline{B})^{1/2}(1-h)\right). \tag{17}$$

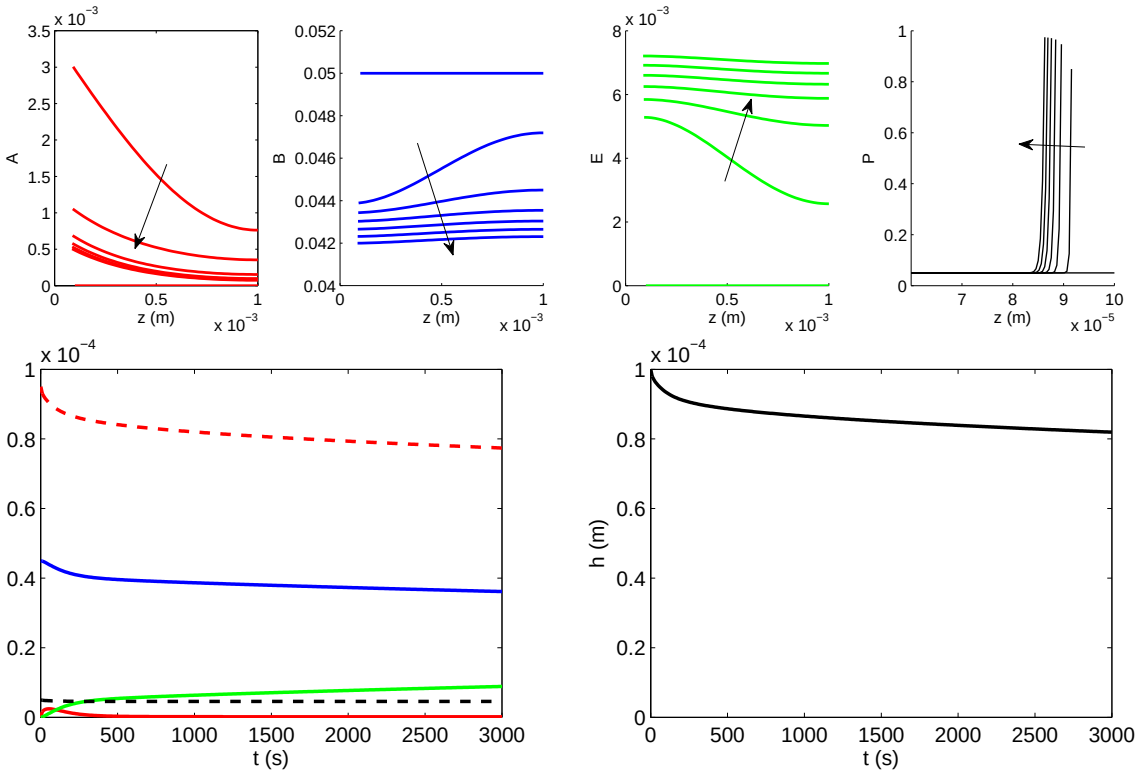

Figure 6: As above, but including an initial 5% polymer in the polymer layer which diffuses with diffusion coefficient $D_P = 10^{-15}$ m^2 s^{-1}. Note that the plotted profiles in A are decreasing over time since, after a quick initial phase in which A diffuses out into the upper layer, the saturated value of $A = \mu A_1$ decreases, as the build up of polymer reduces the value of A_1 at the interface.

We can now substitute this into equation (15) and we obtain

$$(1-h)\overline{B}_\tau = \overline{B}h_\tau - \chi^*(k_1^*\overline{B})^{1/2}\tanh\left((k_1^*\overline{B})^{1/2}(1-h)\right) = \overline{B}h_\tau + \chi^* h_\tau. \quad (18)$$

Integrating this over τ, we have

$$(1-h)\overline{B} - \chi^* h = I_H(\text{a constant}) = 1 - h_0 - \chi^* h_0, \quad (19)$$

since the initial value of B in this scaling is 1.

(2.4.4) It is useful to take this a little further in the case where $k_1^*\overline{B}$ is small. The differential equation (17) for h as a function of τ then is approximately

$$h_\tau = -k_1^*\overline{B}(1-h) = -k_1^*(1 - h_0 - \chi^* h_0 + \chi^* h). \quad (20)$$

Since $h = 0$ initially we have

$$h = h_0 - \frac{(1-h_0)}{\chi^*}\left(1 - \exp(-k_1^*\chi^*\tau)\right). \quad (21)$$

This illustrates two things. First, when $\tau \to \infty$, $h \to h_0 - (1-h_0)/\chi^*$, and so for complete removal of the contaminant we need

$$\frac{\text{moles of A}}{\text{moles of B}} = \frac{\chi^* h_0}{1-h_0} < 1, \tag{22}$$

which is of course, no surprise. Second, if that inequality is satisfied, then this condition shows how the time to reach $h = 0$ (*i.e.* to remove the contaminant completely) depends on the constants involved. In particular we obtain more rapid removal by increasing k_1^* or χ^*, *i.e.* by increasing the reaction rate or the applied concentration. In fact, the time to reach complete removal in this scaling is

$$\tau_{\text{remove}} = -\frac{1}{k_1^* \chi^*} \log_e \left(1 - \frac{\chi^* h_0}{1-h_0}\right), \tag{23}$$

where the second term inside the logarithm is precisely the mole ratio of A:B that we saw above in equation (22).

(2.4.5) The removal time can also be studied numerically by the numerical simulations described earlier. The graphs in Figure 7 show the time at which most of B is used up, as functions of the solubility μ and the reaction rate constant.

2.5 Spherically symmetric model

(2.5.1) If the droplet is taken as initially a hemisphere, and the decontaminant solution is a concentric hemisphere, and the effects of the solid surface are neglected, then the concentrations will remain spherically symmetric. The situation is illustrated in Figure 8. So they will be functions of r and t only, and the only difference from the previous model is to replace z by r, and, for instance, $\partial^2 A/\partial z^2$ by $\partial^2 A/\partial r^2 + (2/r)\partial A/\partial r$ (the Laplacian operator for a spherically symmetric function).

(2.5.2) Surface tension is also neglected in this model, and the contact angle is assumed to remain constant and equal to a right angle. There is assumed to be no pinning of the contact line.

(2.5.3) One effect that may occur in reality but is not taken into account in this model is any attachment of the polymer to the surface. The mathematical model keeps all the polymer still dissolved in A.

(2.5.4) Some numerical results from this model are shown in Figure 9. There is a qualitative similarity between these results and those of Figure 4, however the depletion of decontaminant happens on a shorter timescale. Large values of k_1^* mean that the rate depletion is limited by the speed of diffusion of contaminant. Diffusion will occur quicker in the spherical

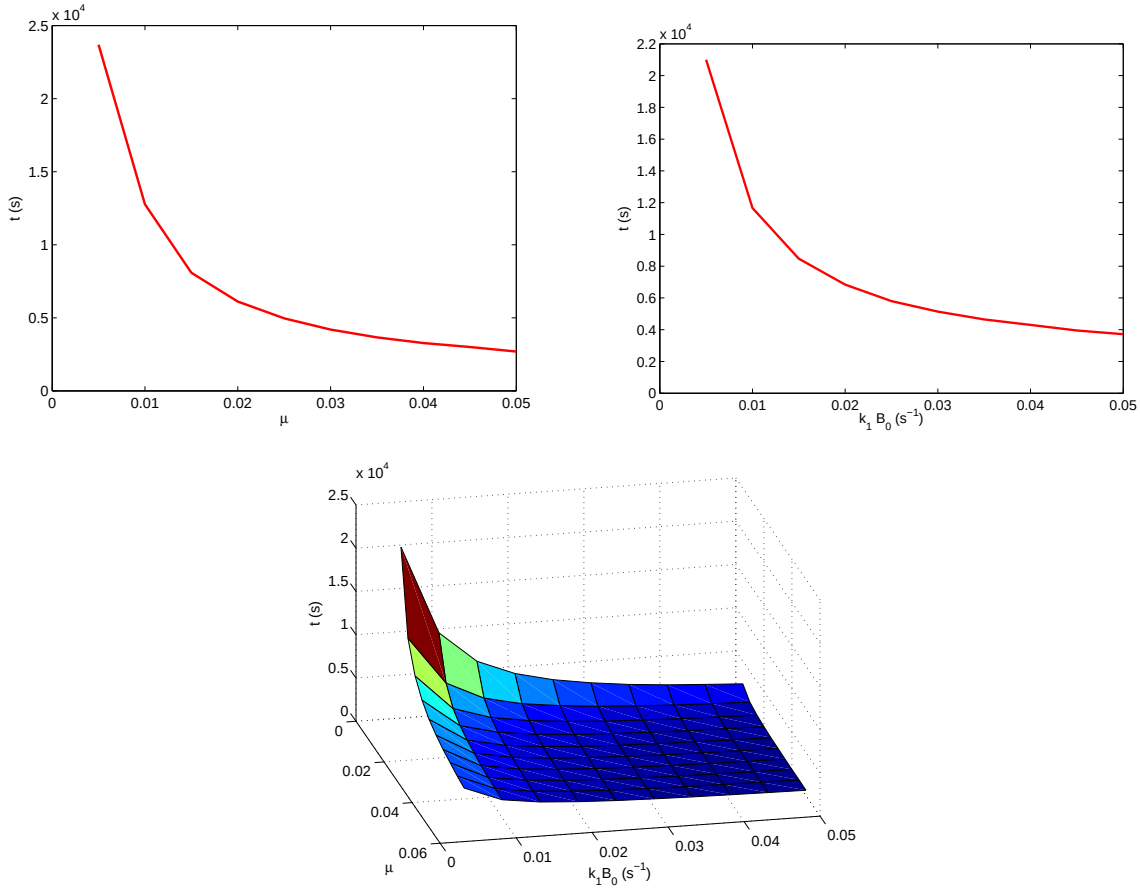

Figure 7: Values of time at which amount of B reaches 10^{-4} of its initial value for various values of reaction rate $k_1 B_0$ (B_0 is initial concentration of B) and solubility ratio μ. These come from numerical solution of reaction diffusion equations for A and B in decontaminant layer, with moving boundary as pollutant is taken up by the decontaminant. The polymer is ignored. $B_0 = 5\%$, $D_A = D_B = 10^{-9}$ m^2 s^{-1}, $h = 0.1$ mm, $H = 1$ mm ($D^* = 1$, $\chi^* = 20$). In the first case $k_1 B_0 = 0.005$ and μ is varied, in the second $\mu = 0.005$ and $k_1 B_0$ is varied, and the third plot shows a two dimensional plot of parameter space.

geometry owing to the larger area for a given volume. This implies that the rate of depletion should be larger for a spherical drop than for a thin layer.

(2.5.5) It would be possible to include polymer in the numerical model in this case but this has not been done here.

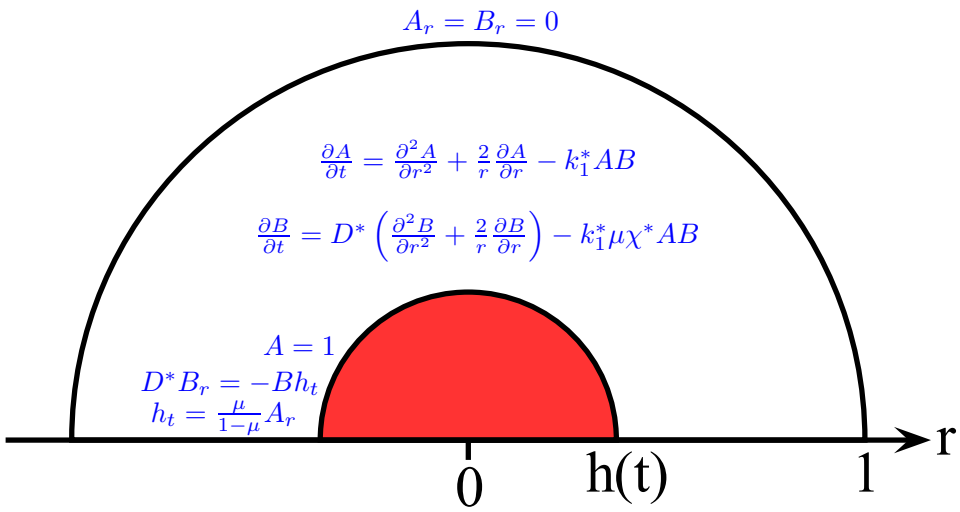

Figure 8: Configuration of the hemispherical model with no polymer. The equations are given in scaled variables.

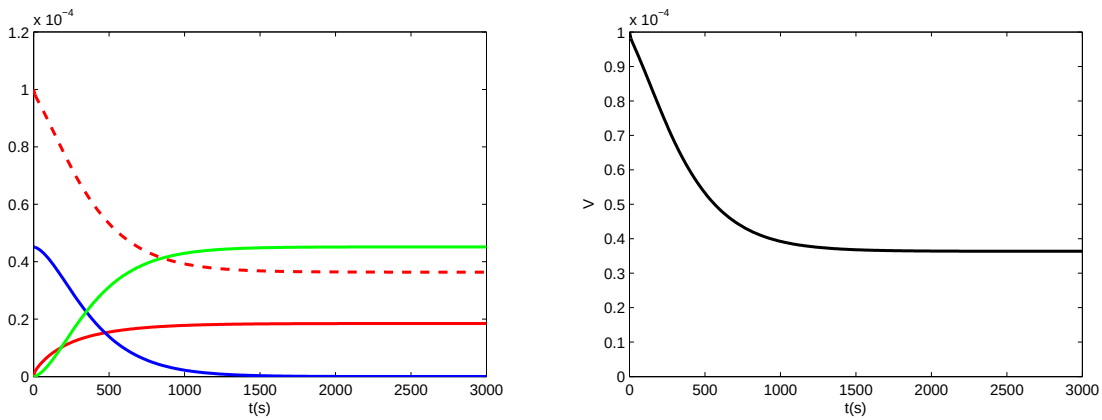

Figure 9: As in Figure 4, but using a spherical geometry. For ease of comparision with the one-dimensional model, the total volume of the layer has again been set to 10 times the initial volume of the drop of contaminant.

2.6 Two-dimensional model

(2.6.1) We now write down the analogous 2-dimensional model, using the same notation as above. We shall consider the situation in Figure 10, so the droplet initially occupies $0 < z < h_0(x)$ for $-L < x < L$, and the applied solution occupies the rest of $-R < x < R$, $0 < z < H$. If the initial shape of the droplet is symmetric about the z-axis, it will remain symmetric at later times, and we shall assume this so we only refer to the region $x > 0$.

(2.6.2) At time t the droplet will occupy $0 < z < h(x,t)$. The unit normal to the

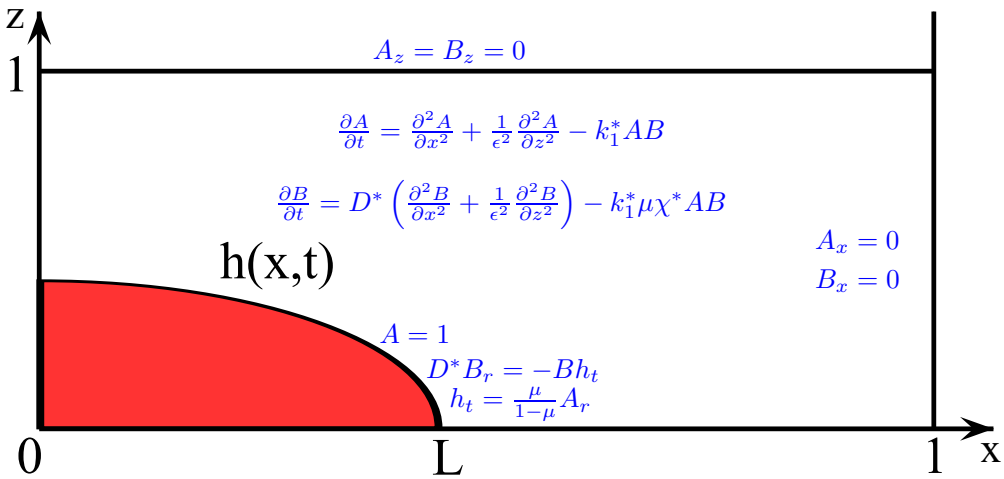

Figure 10: Configuration of the 2-dimensional model, without polymer. The equations are given in scaled variables.

droplet surface is

$$\mathbf{n} = \frac{(-h_x, 1)}{\sqrt{1+h_x^2}}, \tag{24}$$

where we are using h_x and h_t to denote $\partial h/\partial x$ and $\partial h/\partial t$, and we shall use the subscript notation for partial derivatives generally here.

(2.6.3) The diffusion equations for A and B in layer 2 are as before,

$$A_{2t} = D_{A2}(A_{2xx} + A_{2zz}) - k_1 AB, \tag{25}$$
$$B_t = D_B(B_{xx} + B_{zz}) - k_1 AB. \tag{26}$$

The boundary conditions on the upper and lower surfaces are

$$A_{2z} = 0, \quad B_z = 0 \text{ on } z = H; \tag{27}$$
$$A_{1z} = 0 \text{ on } z = 0, \quad 0 < x < L; \tag{28}$$
$$A_{2z} = 0 \text{ on } z = 0, \quad L < x < R. \tag{29}$$

(2.6.4) On the layer interface, we have no transport of B, so the normal derivative $\partial B/\partial n = 0$. The mass transport condition for A analogous to what we had before is

$$-D_{A1}\frac{\partial A_1}{\partial n} + D_{A2}\frac{\partial A_2}{\partial n} = \frac{h_t}{\sqrt{1+h_x^2}}(A_1 - A_2), \tag{30}$$

and we also have $A_2 = \mu A_1$ at the interface as before.

(2.6.5) We take as before initial conditions that the upper layer has $A = 0$, $B = B_0$, and we shall treat the case of no polymer for the moment so $A = A_0 = 1$ in the lower layer. (We therefore drop the suffix 2 from A in the upper layer now.)

(2.6.6) We rescale A with μ, B with B_0, and z and h with H as before. We scale x with R, and we work on the *radial* diffusion timescale so we rescale t with R^2/D_A.

(2.6.7) The diffusion equations then become

$$A_t = A_{xx} + \frac{1}{\epsilon^2} A_{zz} - k_2^* AB, \tag{31}$$

$$B_t = D^* \left(B_{xx} + \frac{1}{\epsilon^2} B_{zz} \right) - k_2^* \mu \chi^* AB, \tag{32}$$

where $\epsilon = H/R$ is the aspect ratio, and $k_2^* = k_1 B_0 R^2/D_A$, which is $k_2^* = k_1^*/\epsilon^2$ in terms of the k_1^* we had in section (2.4). We still have $D^* = D_B/D_A$ and $\chi^* = A_0/B_0 = 1/B_0$ as before.

(2.6.8) The boundary conditions in the scaled variables are $A_z = B_z = 0$ at $z = 1$, and on the interface ($z = h$) we have $A = \mu$ and

$$A_z - \epsilon^2 h_x A_x = \epsilon^2((1-\mu)/\mu) h_t \tag{33}$$

$$B_z - \epsilon^2 h_x B_x = 0. \tag{34}$$

(2.6.9) We now assume k_2^* is of order 1, and ϵ is small. At leading order in ϵ, $A = 1$ above the droplet (*i.e.* in $0 < x < L$), and $A = A(x,t)$ elsewhere, and $B = B(x,t)$ throughout. This is natural since on this timescale the diffusion through the thickness H is fast, and so we are effectively seeing a one-dimensional problem where the activity is in the x-direction and is uniform through the layer thickness. The difference is that the layer thickness varies with x.

(2.6.10) It therefore forms a similar model to that studied in section (2.4). As there, we can obtain the differential equation for B by integrating the leading order term in the B diffusion equation through the layer, and using the upper and lower boundary conditions. In this way we obtain the system

$$B_t = \frac{D^*((1-h)B_x)_x}{1-h} - k_2^* \mu \chi^* AB, \tag{35}$$

$$A_t = A_{xx} - k_2^* AB \quad (x > L) \tag{36}$$

$$A = 1 \quad (x < L). \tag{37}$$

Then if we let $I_H = \mu k_2^*/(1-\mu)$, the droplet thickness h varies according to

$$h_t = -I_H B(1-h), \tag{38}$$

and so

$$h = 1 - (1-h_0) \exp\left(I_H \int_0^t B \, dt \right), \tag{39}$$

until h reaches 0 (at any $x < L$) at which point it stops. When h reaches 0 we no longer have the condition $A = 1$ on the lower interface. The droplet

will of course reach $h = 0$ at different times for different x, so although we have assumed the contact line is pinned, the apparent diameter of the droplet will reduce.

(2.6.11) This model has also been solved numerically for small χ^*. Some results are shown in Figures 11–12. Note that the numerical calculation assumes that a thin film is left behind on the substrate as the contact line retreats, and so mass transfer of A occurs for $x < L$ at all times.

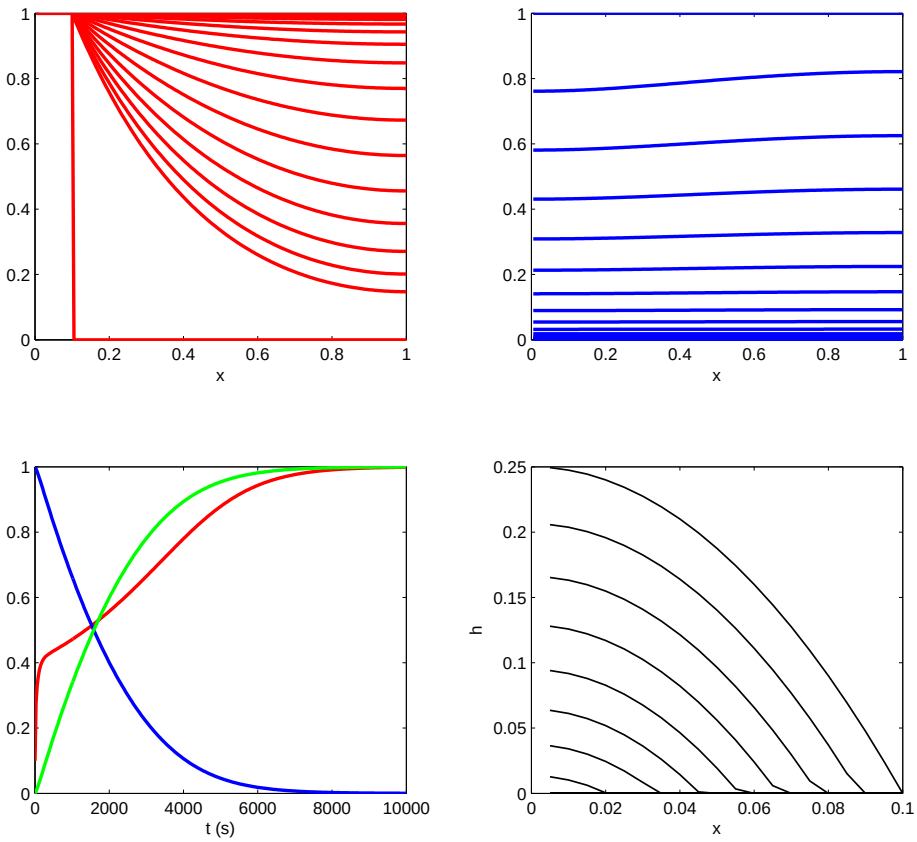

Figure 11: Numerical results for the two-dimensional model using $\mu = 0.02$, $D^* = 1$, $\chi^* = 5$, $k_2^* = 10$. The initial drop profile is parabolic with aspect ratio 4, and with radius $L = 0.1$. As the drop size decreases, a thin film of fluid is assumed to be left on the substrate, which acts as a constant source of contaminant. The long time behaviour is therefore depletion of decontaminant via diffusion from a constant source at $x < L$.

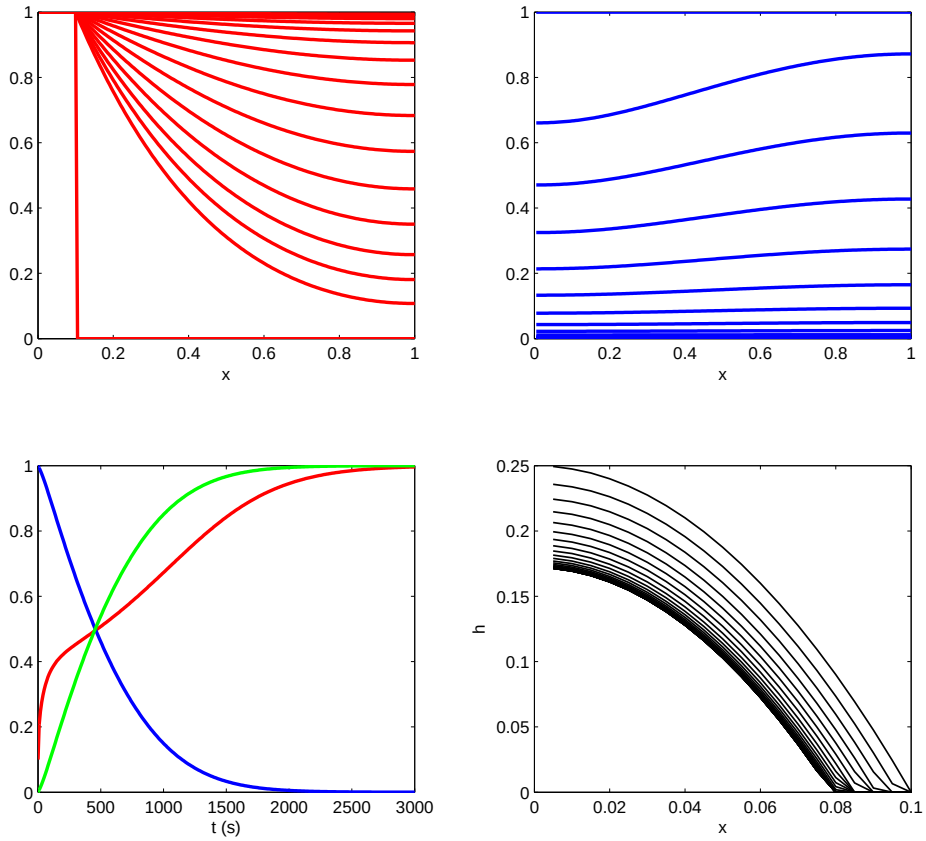

Figure 12: As in Figure 11, but with $\chi^* = 20$. The decontaminant in this case is depleted before the drop is exhausted. Although the behaviour is qualitatively similar to that shown in Figure 11, the timescale is shorter owing to the enhanced diffusion of B within the thinner layer above the drop.

2.7 Models with flow

(2.7.1) In cases where the droplet is on a vertical surface, the model has to have fluid flow with velocity $\mathbf{u}$. So we shall have advection-reaction-diffusion equations of the form

$$\frac{\partial A}{\partial t} + \mathbf{u}.\nabla A = D_A \nabla^2 A - k_1 AB, \tag{40}$$

$$\frac{\partial B}{\partial t} + \mathbf{u}.\nabla B = D_B \nabla^2 B - k_1 AB. \tag{41}$$

The flow inside the droplet will also need to be modelled, and the surface tension will come in, and there will need to be models for the contact line motion.

(2.7.2) To write this down in more detail we take a two-dimensional model with a slope of angle α (90° for a vertical surface) and axes as in Figure 13 with x downslope and z perpendicular. So we write the fluid velocity as $\mathbf{u} = (u, w)$. We shall write $\mathbf{u} = \mathbf{u}_1$ in layer 1, and $\mathbf{u} = \mathbf{u}_2$ in layer 2. Each flow is incompressible so $\partial u/\partial x + \partial w/\partial z = 0$.

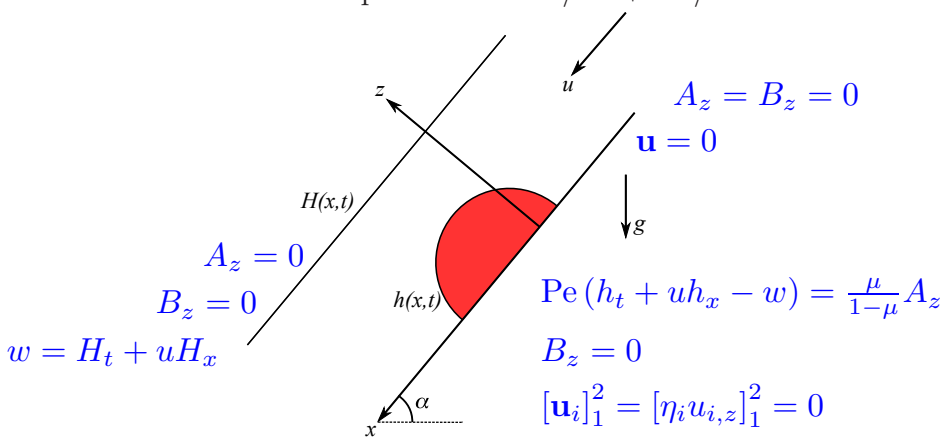

$$\mathrm{Pe}\left(\frac{\partial A}{\partial t} + (\mathbf{u_2}\cdot\nabla)\,A\right) = \frac{\partial^2 A}{\partial z^2} - k_1^* AB \qquad \mathrm{Pe}\left(\frac{\partial B}{\partial t} + (\mathbf{u_2}\cdot\nabla)\,B\right) = D^*\frac{\partial^2 B}{\partial z^2} - k_1^*\mu\chi^* AB$$

$$\frac{\partial p_1}{\partial x} = \eta^*\frac{\partial^2 u_1}{\partial z^2} + 1 \qquad \frac{\partial p_2}{\partial x} = \frac{\partial^2 u_2}{\partial z^2} + 1$$

$$\frac{\partial p_1}{\partial z} = 0 \qquad \frac{\partial p_2}{\partial z} = 0$$

Figure 13: Configuration for the sloping model with flow.

(2.7.3) Then the scaled slow flow equations in layer 1 are

$$0 = -\frac{p_{1x}}{\epsilon^2} + \left(u_{1xx} + \frac{u_{1zz}}{\epsilon^2}\right) + \frac{\mathrm{St}}{\epsilon^2}\sin\alpha, \tag{42}$$

$$0 = -\frac{p_{1z}}{\epsilon^3} + \epsilon\left(w_{1xx} + \frac{w_{1zz}}{\epsilon^2}\right) - \frac{\mathrm{St}}{\epsilon^2}\cos\alpha. \tag{43}$$

Here the Stokes number is $\mathrm{St} = \rho g H^2/(\mu U)$ where U is the velocity scale, μ the viscosity, ρ the density, and ϵ is the aspect ratio of the droplet (height:radius), which is assumed small.

(2.7.4) The boundary conditions on $z = 0$ are $\mathbf{u}_1 = 0$ where the droplet sits. On the interface, $\mathbf{u}_1 = \mathbf{u}_2$, and the mass balance equation written before needs to be modified to include the advective fluxes. The pressures in the layers will be related by $p_2 - p_1 = \gamma h_{xx}$ where γ is the interfacial surface tension.

(2.7.5) In layer 2 we have the same equations for u_2 and w_2 as we wrote for u_1 and w_1. Where layer 2 reaches the substrate we have $\mathbf{u}_2 = 0$. At the

upper surface, $z = H(x,t)$, we have $\partial u_2/\partial z = 0$, $w_2 = H_t + u_2 H_x$, and $p_2 = -\gamma_2 H_{xx}$ where γ_2 is the surface tension of layer 2 in air.

(2.7.6) Although we have not made any progress with solving these equations, they will allow the study of how the timescale of diffusive transport of B *through* the layer compares with its advection *past* the droplet. The B remaining in layer 2 will then be mixed in the flow downstream of that droplet and so will be available to react with a droplet lower down the slope, but at a reduced concentration.

(2.7.7) In fact, taking U to be the velocity scale for steady flow down the slope, the Peclet number $\mathrm{Pe} = UH/D_A$ is estimated as 6000, indicating that the flow down the slope is too fast for diffusion into the droplet to have significant effect. This very much agrees with observations by Dstl that if a fine mist is sprayed onto the surface then much less fluid is needed than if it is sprayed on in such a way that it runs down.

3 Conclusions

(a) Certainly it is essential to ensure that there is enough *mass* of decontaminant to react with all the contaminant.

(b) It is also essential to ensure that the decontaminant has enough *time* in contact.

(c) Mathematical models of the decontamination process have been written for various cases.

(d) These models can, depending on parameter values, show the observed effect of the formation of a polymer "skin" that can prevent the complete removal of A.

(e) The calculations for flow down a slope indicate that the flow is too fast for the necessary diffusive transport of B to the interface. This is in accordance with Dstl's observation that a fine mist, providing a thin layer that does not flow down the surface, is able to decontaminate using less fluid than when there is flow.

We should also point out various areas that we have not investigated in this study:

(a) We have only included the simple one-step reaction between A and B, whereas it is thought that in reality the oxidation of A is more complex.

(b) We have not included any realistic model for the rheology of the polymer P, or the flow of A through it when P begins to concentrate near the interface.

(c) We have not considered the effects of the interaction of the decontaminating solution with *multiple* droplets.

(d) We have not considered the case where B is dissolved in a microemulsion, in which case there is dissolution of the organic components into the contaminant, with consequent swelling of the polymer.

4 Representative data values

Dstl have carried out experiments of various kinds which we report briefly here, along with the other data values that have been used in the numerical simulations.

4.1 Reaction rate experiment

(4.1.1) The reaction rate constant has been estimated by a reaction in which B is present at a concentration that does not reduce much during the time that [A] is halved, and the time for that halving is measured.

(4.1.2) The decontamination reagent that we have called B is an oxidising agent. In its raw form it is sodium dichloroisocyanurate dihydrate, sold commercially as fichlor.[1] This dissolves in water to produce hypochlorite ions ClO^-. In fact each mole of fichlor produces 2 moles of ions. The molecular weight of fichlor is 255.98. (But note that some of Dstl's calculations appear to have used the anhydrous molecular weight of 219.95.) We shall regard the hypochlorite ions as the reagent B, so the ionic weight is 51.4.

(4.1.3) In the reaction rate experiment, 4.6 g fichlor were dissolved in 100 ml of water. This gives a concentration of B of 0.03594 moles/100 ml (based on the molecular weight of the hydrated form). The typical concentration of B in solution is that resulting from this concentration of 4.6 g of fichlor to 100 ml of water, which is a little less than 2% by weight of hypochlorite ions (our reagent B).

(4.1.4) In the reaction rate experiment, the contaminating agent A had molecular weight 159.1, density 1.274 gm/cc, viscosity 3.95 cP, solubility in water 0.06 g/100 ml, and surface tension 42.5 dyne/cm. It was dissolved with 200 μl in 25 ml of solution. This gives a concentration of 0.6406 moles/100 ml.

(4.1.5) When a microemulsion is used, the solubility of A can rise to 0.25 or even 0.95 (*i.e.* 95 g of A in 100 g of water).

(4.1.6) The polymer used in this experiment had average molecular weight 2×10^6, being composed of on average 2×10^4 monomers each of molecular weight 100.

[1] The formula, structure and details are available from `http://www.chemblink.com/products/51580-86-0.htm`.

(4.1.7) The observed time for the concentration of A to halve was $T_h = 6\,\text{sec}$. In terms of a pseudo-first-order reaction rate constant K_{obs} such that $dA/dt = -K_{\text{obs}}A$, this means that $K_{\text{obs}} = \log_e 2/T_h$. In terms of the constant in a reaction rate equation of the form $dA/dt = -KAB$, this means that $KB = K_{\text{obs}}$ where B is the concentration of B during the experiment (treated as constant).

4.2 Droplet decontamination experiments

(4.2.1) In other experiments, contaminant droplets of measured weight were placed on a metal plate, the reagent washed off, and the residual amount of contaminant estimated by extracting it to a solvent. (The droplets were much larger than those that would be produced by an aerosol.) This was then repeated with droplets of similar size but leaving the reaction to proceed for 30 or 60 or 120 minutes.

(4.2.2) The initial drop radius on the plate was estimated. Part of this table of data is shown.

Drop radius (mm)	No. of drops	Wgt tHD (mg)	Decon. time mins	% reco--very	mass (mg)	r (mm)
4.5	1	46.1510	15	77.09	33.0755	3.946
	1	47.6995	30	68.92	30.5595	3.850
etc.	...	...	...	...	...	...
	1	52.0790	Control	107.57	52.7090	4.539

In this, the Wgt column is the mass of A+P in mg, and P was present at 5% by weight, and this was placed in a Petri dish, and decontaminant added. Then at a time of say 15 minutes, the plate was removed, The % recovery column is the proportion of the mass of A that remained after the stated time, compared to the initial mass of A. In the final column labelled r, this has been converted to an "equivalent" drop radius using a fit (derived from other experimental data on droplets of this kind) in which volume is proportional to the 3.2 power of radius. The "Control" line is for a droplet that was deposited and then no reaction was carried out, but the content was estimated in the same way as was done in the other cases. These often give overestimates (as above) of the amount of A present.

(4.2.3) It may be possible to correct for this but it has not been done systematically in the table. In fact for the 1 drop case the first value of the control recovery has been used to rescale each of the other cases, and 100% has been used for the cases of 2, 4, 8 drops.

(4.2.4) Some of the estimated values of A after 120 minutes may be incorrect, because the polymer is observed to form a seal over whatever is left, and

it may be that in some cases this has prevented all of the A from being extracted by the solvent.

(4.2.5) The depth of reagent that was added in these experiments is not known exactly, but was such that the reagent just covered the drops. The Petri dish diameter is 11.5 cm (radius 5.75 cm) the metal plate is 8 mm×5 mm×0.2 mm, and it is believed that 20 or 25 ml of reagent were added. These would give depths of about 0.7 mm or 1.2 mm above the top of the plate.

4.3 Delivery rate experiments

(4.3.1) In these experiments, contaminant droplets were put on metal plates, which were mounted vertically, sprayed for say 10 seconds, left for 15 minutes, and the residual A estimated. It was found that the jet velocity was important rather than the coverage in volume delivered. This was in a context where the reagent was delivered in a microemulsion. Dstl's suggestion for how the velocity of delivery might affect the process was that the jet may partly flatten the droplets, and so thin the layer that needs to be removed.

4.4 Diffusivities

(4.4.1) We assume that the diffusivities of the species in aqueous solution are inversely proportional to $M^{3/4}$ where M is molecular weight, and we take the diffusivity of oxygen to be $10^{-9}\,\mathrm{m}^2/\mathrm{s}$, so we take

$$D_A = 10^{-9}\left(\frac{159.1}{32}\right)^{-3/4}, \quad D_B = 10^{-9}\left(\frac{51.4}{32}\right)^{-3/4}, \tag{44}$$

both in m^2/s.

Bibliography

[1] Physical models of diffusion for polymer solutions, gels and solids. L. Masaro, X.X.Zhu. Prog. Polym. Sci. 24, 731–775 (1999).

[2] Two phase modelling of air bubbles in ice cream. Study Group report from Bristol 2003, available from `www.smithinst.ac.uk/Projects/ESGI46/ESGI46-IceCream`